0090-9556/02/3009-962–969$7.00
DRUG METABOLISM AND DISPOSITION
Vol. 30, No. 9
689/1003958
DMD 30:962–969, 2002
Printed in U.S.A.

MECHANISMS OF IMPAIRED BILIARY EXCRETION OF ACETAMINOPHEN GLUCURONIDE AFTER ACUTE PHENOBARBITAL TREATMENT OR PHENOBARBITAL PRETREATMENT

HAO XIONG, HIROSHI SUZUKI, YUICHI SUGIYAMA, PETER J. MEIER, GARY M. POLLACK, AND KIM L. R. BROUWER

Division of Drug Delivery and Disposition, School of Pharmacy, University of North Carolina, Chapel Hill, North Carolina (H.X., G.M.P., K.L.R.B.); Graduate School of Pharmaceutical Sciences, University of Tokyo, Tokyo, Japan (H.S., Y.S.); and Division of Clinical Pharmacology and Toxicology, Department of Medicine, University Hospital Zurich, Zurich, Switzerland (P.J.M.)

(Received January 24, 2002; accepted May 28, 2002)

This article is available online at http://dmd.aspetjournals.org

ABSTRACT:

Previous studies have demonstrated that phenobarbital (PB) significantly impairs the biliary excretion of acetaminophen glucuronide (AG) in rats. Studies also suggested that Mrp2 mediates AG biliary excretion, and Mrp3 is involved in AG basolateral export. It was hypothesized that inhibition of Mrp2-mediated AG transport by PB or PB metabolites, and PB induction of Mrp3, may contribute to the impaired biliary excretion of AG by PB. In the present study, the hepatobiliary transport of AG in single-pass isolated perfused Wistar and TR$^-$ rat livers was investigated. The AG biliary clearance was markedly decreased, and the AG basolateral clearance was significantly increased in TR$^-$ rat livers. Uptake of AG by Mrp2 and Mrp3, and inhibition of Mrp2- and Mrp3-mediated transport by PB and major PB metabolites, were investigated with rat Mrp2- or Mrp3-expressing Sf9 cell plasma membrane vesicles (Sf9-PMVs). AG was transported by Mrp3 ($K_m \approx 0.91$ mM). Net ATP-dependent AG uptake into Mrp2-expressing Sf9-PMVs could not be detected directly. However, AG significantly inhibited Mrp2-mediated 5-(and 6)-carboxy-2′,7′-dichlorofluorescein (CDF) transport. *p*-Hydroxyphenobarbital glucuronide (*p*-OHPBG), but not PB or *p*-hydroxyphenobarbital, significantly inhibited Mrp2-mediated CDF transport. The IC_{50} values for *p*-OHPBG inhibition of Mrp2-mediated CDF uptake and Mrp3-mediated AG transport were similar (~0.68 and 0.46 mM, respectively). PB treatment (80 mg/kg/day × 4 days) markedly increased hepatic Mrp3 expression in Wistar rats. In conclusion, inhibition of Mrp2-mediated AG transport by *p*-OHPBG provided one possible explanation for the impaired biliary excretion of AG after acute PB treatment. However, impaired biliary excretion of AG after PB pretreatment may be attributed primarily to the induction of hepatic Mrp3 by PB.

Acetaminophen glucuronide (AG[1]), a monovalent organic anion formed in hepatocytes following acetaminophen (APAP) administration, undergoes both biliary excretion and basolateral export from hepatocytes. Approximately 50% of AG formed in hepatocytes is excreted in bile; the remainder traverses the basolateral membrane into blood and undergoes renal elimination. AG excretion in bile accounts for ~7% of the administered APAP dose (100 mg/kg) in rats in vivo (Brouwer and Jones, 1990) and ~10% in the isolated perfused rat liver at equivalent APAP concentrations (Studenberg and Brouwer, 1992; Turner and Brouwer, 1997). Pretreatment with phenobarbital (PB), a common enzyme-inducing agent, significantly increased AG formation but impaired AG biliary excretion 3- to 6-fold in the rat in vivo (Brouwer and Jones, 1990) and in the isolated perfused rat liver (Studenberg and Brouwer, 1992). Acute PB treatment also markedly (~3-fold) decreased the biliary excretion of AG along with a moderate reduction (~1.5-fold) in AG formation (Studenberg and Brouwer, 1992).

Several distinct mechanisms may be involved in decreased biliary excretion of AG after PB treatment. Previous studies suggested that the decrease in APAP glucuronidation may contribute in part to the impaired biliary excretion of AG after acute PB treatment. Intracellular sequestration of AG does not play a role in the reduction in AG biliary excretion after either PB pretreatment or acute PB treatment (Studenberg and Brouwer, 1992, 1993). PB is a well-known enzyme inducer that also induces hepatocyte basolateral transporters, multidrug resistance-associated protein 3 (Mrp3; Abcc3), and organic anion transporting polypeptide 2 (Oatp2; Slc21a5), in Sprague-Dawley rats (Ogawa et al., 2000; Rausch-Derra et al., 2001). PB pretreatment may

This work was supported by National Institutes of Health Grant GM41935. It was presented in part at the American Association of Pharmaceutical Scientists annual meeting, 2001, October 21–25, Denver, CO and was submitted to the Graduate School of the University of North Carolina in partial fulfillment of requirements for the Doctor of Philosophy degree in Pharmaceutical Sciences (H.X.).

[1] Abbreviations used are: AG, acetaminophen glucuronide; APAP, acetaminophen; PB, phenobarbital; Mrp, multidrug resistance-associated protein; *p*-OHPB, *p*-hydroxyphenobarbital; *p*-OHPBG, *p*-hydroxyphenobarbital glucuronide; AS, acetaminophen sulfate; TR$^-$, Mrp2 transport-deficient; PMV, plasma membrane vesicle; TC, taurocholate; CDF, 5-(and 6)-carboxy-2′,7′-dichlorofluorescein; HPLC, high-performance liquid chromatography; $E_2 17\beta$G, estradiol 17β-glucuronide; GFP, green fluorescence protein; Oatp, organic anion transporting polypeptide.

Address correspondence to: Kim L. R. Brouwer, Pharm.D., Ph.D., Division of Drug Delivery and Disposition, School of Pharmacy, CB 7360, Beard Hall, University of North Carolina at Chapel Hill, Chapel Hill, NC 27599-7360. E-mail: kbrouwer@unc.edu

impair the biliary excretion of AG via up-regulation of one or more AG basolateral export transporters in rat liver.

In rats, the half-life of PB is ~9 h (Brouwer et al., 1984). PB is metabolized in the liver by cytochrome P450 enzymes to *p*-hydroxyphenobarbital (*p*-OHPB), which is metabolized further primarily to *p*-hydroxyphenobarbital glucuronide (*p*-OHPBG). In rats with bile fistula, approximately 20 to 30% of the PB dose recovered in bile was the parent compound, and 50 to 60% was free or conjugated *p*-OHPB (mainly *p*-OHPBG) (Levin et al., 1986). The transport mechanisms for biliary excretion of PB, *p*-OHPB, and *p*-OHPBG have not been clarified. It was hypothesized that *p*-OHPB or *p*-OHPBG may share a canalicular transporter with AG and that one or both of these metabolites competitively inhibit the biliary excretion of AG after acute PB treatment.

Previous pharmacokinetic modeling of data obtained from recirculating isolated perfused rat liver studies suggested that the biliary excretion of AG is mediated almost exclusively by Mrp2 (Abcc2) and that Mrp3 is involved in the basolateral export of AG (Xiong et al., 2000). In the present study, the disposition of APAP, AG, and acetaminophen sulfate (AS) was studied further in single-pass isolated perfused Wistar control and Mrp2 transport-deficient (TR^-) rat livers, and the basolateral clearance of AG and biliary clearances of AG and AS were calculated directly. ATP-dependent uptake of AG into plasma membrane vesicles (PMVs) prepared from Sf9 insect cells transiently transfected with recombinant rat *Mrp2* or *Mrp3* was examined to confirm the roles of Mrp2 and Mrp3 in the transport of AG across liver canalicular and basolateral membranes, respectively. The inhibition of Mrp2- or Mrp3-mediated transport by PB, *p*-OHPB, and *p*-OHPBG was examined in vitro in Sf9 cell PMVs. Finally, the effect of PB pretreatment on the hepatic expression of Mrp2 and Mrp3 was examined.

Materials and Methods

Reagents. APAP, AG, taurocholate (TC), PB, and *p*-OHPB were purchased from Sigma-Aldrich (St. Louis, MO). AS was a gift from McNeil Pharmaceuticals (Ft. Washington, PA). 5-(and 6)-Carboxy-2′,7′-dichlorofluorescein (CDF) was obtained from Molecular Probes, Inc. (Eugene, OR). *p*-OHPBG was synthesized enzymatically as described by Studenberg et al. (1995) and was >99% pure as determined by HPLC. [^{3}H]AG (12.4 Ci/mmol) was synthesized by Amersham Biosciences UK, Ltd. (Little Chalfont, Buckinghamshire, UK) and was >99% pure as determined by HPLC. [^{3}H]Estradiol 17β-glucuronide ($E_2$17βG) (44 Ci/mmol) and [^{3}H]TC (2.4 Ci/mmol) were purchased from PerkinElmer Life Sciences (Boston, MA). All other chemicals were of analytical reagent grade. Anti-Mrp3 antiserum was raised in Dr. Yuichi Sugiyama's laboratory (Tokyo, Japan). Anti-Mrp2 antibody was generated in Dr. Peter Meier's laboratory (Zurich, Switzerland). Anti-mouse actin antibody was purchased from Chemicon International Co. (Temecula, CA).

Animals. Male Wistar rats were obtained from Charles River Laboratories Inc. (Raleigh, NC). Male TR^- rats hereditarily deficient in Mrp2 protein were bred in our animal facility. Rats were maintained on a 12-h light/dark cycle. Access to rat chow and water was allowed ad libitum. Rats were allowed to acclimate for at least 5 days prior to experimentation. The Institutional Animal Care and Use Committee of the University of North Carolina at Chapel Hill approved all procedures.

Single-Pass Rat Liver Perfusion. Following anesthesia (ketamine, 60 mg/kg and xylazine, 12 mg/kg, i.p.), livers from male Wistar or TR^- rats (255–275 g) were isolated and perfused with oxygenated Krebs-Ringer bicarbonate buffer containing 3.3 μM taurocholate (pH 7.4) at a flow rate of 30 ml/min in a single-pass perfusion system as described by Vore et al. (1996). The liver was maintained at 36.5 ± 0.5 °C. The bile duct was cannulated with PE-10 tubing. The liver was allowed to equilibrate with the perfusion buffer for ~15 min prior to the administration of APAP. To achieve steady-state quickly, the liver was first perfused with buffer containing 100 μg/ml APAP for 10 min and then perfused with buffer containing 50 μg/ml APAP for an additional 40 min. Bile and outflow perfusate were collected at 10-min intervals during the first 30 min and at 5-min intervals thereafter. After each perfusion, liver homogenate (25% w/v) in 15 mM phosphate buffer (pH 7.4) containing 250 mM sucrose was prepared for the determination of intrahepatic concentrations of APAP, AG, and AS. The liver homogenate also was used to determine the hepatic expression of Mrp3. Bile volume was determined gravimetrically, assuming a density of 1.0. All samples were stored at −20°C until assayed.

Assuming that the liver is a well-stirred compartment and transport across liver canalicular or basolateral plasma membrane occurs in one direction, the excretion rate and excretion clearance of APAP, AG, and AS in the single-pass isolated perfused rat liver were calculated as follows:

$$R_{bile} = C_{bile} \times Q_{bile} \quad (1)$$

$$R_{B/L} = C_{outflow} \times Q_{perf} \quad (2)$$

$$CL_{bile} = \frac{R_{bile}}{C_{liver}} \quad (3)$$

$$CL_{B/L} = \frac{R_{B/L}}{C_{liver}} \quad (4)$$

where R_{bile} and $R_{B/L}$ represent biliary and basolateral excretion rates, respectively; C_{bile}, $C_{outflow}$, and C_{liver} represent drug concentrations in bile, outflow perfusate, and liver, respectively; Q_{bile} and Q_{perf} represent bile and perfusate flow rates, respectively; CL_{bile} and $CL_{B/L}$ represent biliary clearance and basolateral clearance, respectively. CL_{bile} and $CL_{B/L}$ were calculated when the disposition of AG and AS reached steady-state, defined as constant concentrations in the liver and determined by constant biliary and basolateral excretion rates of AG and AS. The steady-state biliary and basolateral excretion rates for AG and AS were calculated as the average of R_{bile} or $R_{B/L}$ values measured after the disposition of AG and AS reached steady-state. C_{liver} for AG and AS was determined as the total amount of each species in the liver at the end of each perfusion divided by the intracellular volume of the liver, which was assumed to be 0.7 ml/g liver (Tsuji et al., 1983; Studenberg and Brouwer, 1993; Takenaka et al., 1995).

PB Treatment and Liver Crude Membrane Preparation. Wistar rats were treated with PB (80 mg/kg, i.p.) or saline daily for 4 days and sacrificed 24 h after the last dose. Liver crude membrane fractions were prepared as described by Bergwerk et al. (1996).

HPLC Assay. APAP, AG, and AS concentrations in bile samples collected from single-pass isolated liver perfusion studies were quantitated by the HPLC method of Brouwer and Jones (1990). Concentrations of APAP, AG, and AS in perfusate and liver homogenate obtained from single-pass perfusion studies were determined by a modified HPLC method. Briefly, aliquots (500 μl) of perfusate samples were evaporated to dryness and reconstituted in 50 μl water. Concentrated perfusate samples (10×), liver homogenate samples (25% w/v), and standards (50 μl) were prepared for analysis by adding 312 μl of 20% acetonitrile and 500 μl of cold acetonitrile containing 44 μg/ml para-aminobenzoic acid. Samples were mixed by vortex, centrifuged, and the supernatant was removed and evaporated to dryness before reconstitution with mobile phase. The mobile phase consisted of 0.4% acetonitrile and 0.75% acetic acid in 25 mM potassium phosphate buffer (final pH 3.14). Standard curves were linear ($r \geq 0.998$) for APAP, AG, and AS in the following concentration ranges: APAP (0.033–0.66, 0.33–6.6, and 0.33–3.3 mM in liver homogenate, perfusate, and bile, respectively), AG (0.014–0.286, 0.014–0.286, and 0.716–7.16 mM in liver homogenate, perfusate, and bile, respectively) and AS (0.018–0.36, 0.036–0.72, and 0.18–1.8 mM in liver homogenate, perfusate, and bile, respectively).

Production of Recombinant Baculovirus. Recombinant pFASTBAC1 plasmids containing either rat Mrp2-, Mrp3-, or green fluorescence protein (GFP)-coding sequence were constructed in Dr. Yuichi Sugiyama's laboratory (University of Tokyo, Tokyo, Japan). The construction of plasmid containing the Mrp2-coding sequence was described by Ito et al. (2001). Recombinant baculovirus was generated with BAC-TO-BAC baculovirus expression system (Invitrogen, Carlsbad, CA). Briefly, pFASTBAC1 recombinant plasmids were transformed first into competent DH10BAC cells containing bacmids and help plasmids. *Escherichia coli* colonies with recombinant bacmids were selected on Luria Agar plates containing 50 μg/ml kanamycin, 7 μg/ml gentamicin, 10 μg/ml tetracycline, 100 μg/ml Bluo-gal, and 40 μg/ml isopropylthio-D-galacotoside. Purified recombinant bacmid DNA was used to transfect Sf9 insect

cells in the presence of CELLFECTIN reagent. Recombinant baculovirus was harvested in the supernatant of cell culture medium after 3 days of culture at 27°C. Recombinant baculovirus stocks ($>10^7$ pfu/ml) were stored at 4°C. The viral titer of each stock was determined by plaque assays.

Viral Infection of Sf9 Insect Cells and Preparation of Plasma Membrane Vesicles. Sf9 insect cells (Invitrogen) were cultured at 27°C in spinner flasks with Grace's insect cell medium (Invitrogen) supplemented with 5% fetal bovine serum, 3.33 g/l lactalbumin hydrolysate, 3.33 g/l yeastolate, and antibiotics/antimycotics (containing 100 units/ml penicillin G, 100 μg/ml streptomycin sulfate, and 0.25 μg/ml amphotericin B; Sigma-Aldrich). Log phase Sf9 cells ($1.0–1.5 \times 10^6$ cells/ml) were infected with recombinant baculovirus at multiplicity of infection between 3 to 5 and were harvested 3 days later. Plasma membrane vesicles were prepared as described by Huang et al. (1998).

Western Blot Analysis. Liver homogenate (80 μg of protein) prepared after single-pass perfusion, liver crude membrane fraction (60 μg of protein), isolated Sf9 cell plasma membrane vesicles or liver canalicular membrane vesicles (15 μg of protein) were separated on 4 to 12% Bis-Tris polyacrylamide gels and transferred to PVDF membranes. The membranes were probed with anti-Mrp2 or anti-Mrp3 antiserum. Positive protein bands were detected with LumiGluo chemiluminescent substrate kit (Kirkegaard and Perry Laboratories, Gaithersburg, MD). The same membrane then was stripped according to the manufacturer's directions (LumiGluo Chemiluminescent reagent kit) and reprobed with anti-mouse actin antibody.

PMV Uptake Studies. Substrate uptake into PMVs was measured by a quick filtration technique (Xiong et al., 2000). Briefly, frozen membrane suspensions were thawed quickly in a 37ºC water bath and passed repeatedly (15×) through a 27-gauge needle. Aliquots of membrane suspensions (20 μl; 20–40 μg of protein) were preincubated for 5 min at 37ºC, and uptake was initiated by the addition of 80 μl of prewarmed incubation medium to the membrane suspensions. The incubation buffer consisted of 20 mM HEPES (pH 7.5), 100 mM potassium nitrate, 100 mM sucrose, 5 mM hemimagnesium gluconate, 0.5 mM hemicalcium gluconate, ATP-regenerating system (10 mM phosphocreatine, 100 μg/ml creatine phosphokinase, and 10 mM $MgCl_2$), and 4 mM of ATP or AMP. Membrane vesicle uptake was terminated by adding 3.5 ml of ice-cold membrane suspension buffer. Vesicle-associated substrate was separated from free substrate by rapid filtration through a 0.45-μM HAWP25 filter (Millipore Corporation, Bedford, MA). Filters were rinsed twice with 3.5 ml of ice-cold membrane suspension buffer. For radiolabeled substrates, filters were immersed in 5 ml of liquid scintillation cocktail and assayed for radioactivity. For CDF, filters were washed in 2 ml of lysis buffer (phosphate-buffered saline containing 0.5% Triton X-100) for 20 min at room temperature. Fluorescent intensity in the lysis buffer was measured with a fluorometer. Nonspecific binding of substrates to the filter was determined in the absence of membrane vesicles. These values were subtracted from all determinations. Net ATP-dependent substrate uptake was calculated by subtracting the uptake in the presence of AMP from that in the presence of ATP. Mrp2- or Mrp3-mediated substrate uptake was calculated as the difference between net ATP-dependent substrate uptake into Mrp2- or Mrp3-expressing Sf9 cell PMVs and control (GFP-expressing) PMVs.

Inhibition Studies. The inhibition of Mrp2-mediated CDF uptake by AG, PB, *p*-OHPB, or *p*-OHPBG was determined by subtracting the net ATP-dependent uptake of 10 μM CDF into control PMVs from that into Mrp2-expressing Sf9 cell PMVs at designated inhibitor concentrations. Likewise, the inhibition of Mrp3-mediated AG uptake by PB, OHPB, or *p*-OHPBG was determined by subtracting the net ATP-dependent uptake of 10 μM AG into control PMVs from that into Mrp3-expressing Sf9 cell PMVs in the presence of each inhibitor. The concentration-dependent inhibition of Mrp2-mediated CDF uptake and Mrp3-mediated AG uptake by *p*-OHPBG was determined with 10 μM CDF and AG, respectively, in the presence of 0 to 1 mM *p*-OHPBG. The potency of *p*-OHPBG to inhibit Mrp2- or Mrp3-mediated transport was determined from the IC_{50} value estimated by nonlinear regression (WinNonlin 1.1; Pharsight Corporation, Mountain View, CA) of the dose-response equation:

$$\frac{v_i}{v_0} = \frac{1}{1 + \left(\frac{[I]}{IC_{50}}\right)^n} \quad (5)$$

where v_i is the transport rate in the presence of inhibitor at concentration [I] and v_0 is the transport rate in the absence of inhibitor; IC_{50} is the inhibitor concentration associated with 50% inhibition; n is the Hill coefficient.

Statistics. The two-tailed Student's *t*-test was used to determine statistically significant differences between the control and TR^- livers with respect to the total recovery, the hepatic concentration, the excretion rates, and the calculated clearance values of AG and AS. For multiple comparisons, analysis of variance was performed to test the statistical difference among all treatment groups. If a difference was found, a paired two-tailed Student's *t* test with Bonferroni correction was conducted between control and each treatment group. The relationship between AG basolateral clearance data and the expression levels of Mrp3 was examined by orthogonal linear regression. In all cases, data are presented as mean ± S.D., and the criterion for statistical significance was $P < 0.05$, unless specified otherwise.

Results

Single-Pass Liver Perfusion. Livers from TR^- rats (12.0 ± 0.5 g) were slightly but statistically larger than control livers (10.9 ± 0.3 g, $P < 0.05$) even though body weights were similar. The steady-state bile flow rates in TR^- rat livers (0.199 ± 0.006 μl/min/g liver) were significantly lower than in control livers (1.02 ± 0.07 μl/min/g liver, $P < 0.001$).

The disposition of APAP, AG, and AS reached steady-state by ~25 min after starting the APAP infusion (Fig. 1). At steady-state, the elimination of APAP and the formation of AG and AS were similar between Wistar and TR^- rats (Table 1). In Wistar rat livers, the excretion rate of AG into bile and perfusate was similar. In contrast, the AS basolateral excretion rate was much greater than the AS biliary excretion rate. The biliary excretion rates of AG and AS were significantly lower in TR^- relative to Wistar rat livers (~500-fold and ~3-fold, respectively). The basolateral excretion rate of AG was significantly increased in TR^- compared with Wistar rat livers. The basolateral excretion rate of AS was not significantly different between TR^- and Wistar rat livers. The AG concentration in TR^- rat livers was significantly lower than in Wistar controls. In contrast, the AS concentration in TR^- rat livers was significantly higher than in Wistar controls. The calculated biliary clearances of AG and AS in TR^- rat livers were decreased ~170- and ~7-fold, respectively. The basolateral clearance of AG in TR^- rat livers was increased more than 7-fold. The apparent basolateral clearance of AS in TR^- rat livers was decreased ~2-fold (Table 1).

Mrp3 Expression. The expression of Mrp3 in Wistar and TR^- rat livers used in the single-pass isolated perfused liver studies described above was examined by Western blot analysis. Mrp3 expression was barely detected in the homogenate of Wistar rat livers. In contrast, significantly higher and variable levels of Mrp3 were detected in the homogenate of TR^- rat livers (Fig. 2A). The AG basolateral clearance in Wistar and TR^- rat livers, determined by single-pass perfusion, showed significant correlation with the expression levels of Mrp3 in these livers ($r^2 = 0.82$, Fig. 2B).

Expression of Rat Mrp2 and Mrp3 in Transfected Sf9 Cells. Sf9 cells were cultured for 3 days after transfection with recombinant baculovirus containing either rat Mrp2-, Mrp3-, or GFP-coding sequence. The expression of Mrp2 and Mrp3 in PMVs prepared from these cells was examined by Western blot analysis (data not shown). Neither Mrp2 nor Mrp3 was detected in GFP-expressing Sf9 cell PMVs. Mrp2 was expressed abundantly in Mrp2-expressing Sf9 cell PMVs to a level similar to that in canalicular liver plasma membrane vesicles. The molecular weight of the Mrp2 expressed in Sf9 cells was slightly lower than the native form expressed in the rat liver, presumably due to lack of glycosylation. Mrp3 was expressed abundantly only in Mrp3-expressing Sf9 cell PMVs.

PMV Uptake Studies. The activities of Mrp2 and Mrp3 expressed

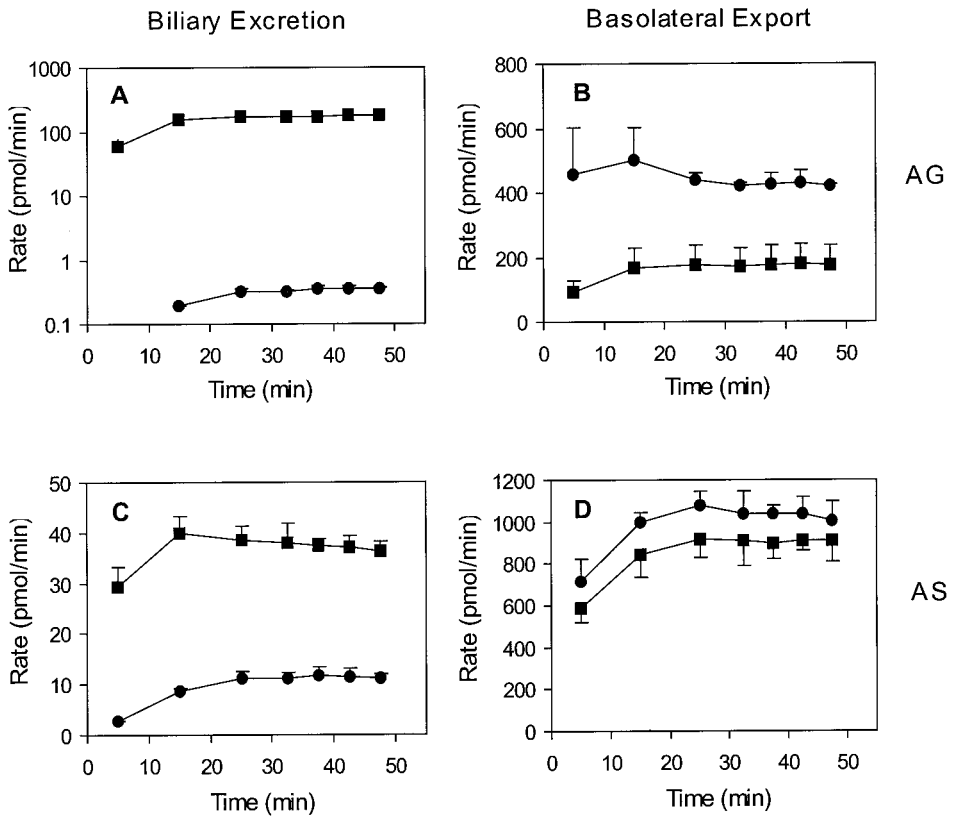

FIG. 1. *Biliary and basolateral excretion rate versus time profiles of AG (A, B) and AS (C, D) in single-pass isolated perfused Wistar (■) and TR⁻ (●) rat livers.* When error bars are not seen, they are smaller than the symbols.

TABLE 1

Hepatobiliary disposition of APAP, AG, and AS in isolated single-pass perfused rat livers at steady-state

R_{bile_AG} and R_{bile_AS} are biliary excretion rates for AG and AS, respectively; R_{B/L_AG} and R_{B/L_AS} are basolateral export rates for AG and AS, respectively; ER is the extraction ratio; AG% and AS% are the percentages of the dose recovered as AG and AS, respectively; C_{liver_AG} and C_{liver_AS} are the AG and AS concentrations at the end of perfusion. CL_{bile_AG}, CL_{bile_AS}, and CL_{B/L_AG} are AG biliary clearance, AS biliary clearance, and AG basolateral clearance, respectively.[a]

	Wistar	TR⁻
Excretion rate (pmol/min)		
R_{bile_AG}	174 ± 11	0.34 ± 0.02*
R_{bile_AS}	37 ± 2	11 ± 1*
R_{B/L_AG}	175 ± 61	428 ± 18*
R_{B/L_AS}	909 ± 85	1039 ± 6
Biotransformation		
ER of APAP	0.30 ± 0.02	0.30 ± 0.02
AG %	12.1 ± 3.3	14.3 ± 0.9
AS %	32.3 ± 2.1	35.2 ± 3.5
Concentration in liver (mM)		
C_{liver_AG}	0.613 ± 0.066	0.415 ± 0.028*
C_{liver_AS}	0.356 ± 0.056	0.526 ± 0.110*
Clearance (μl/min)		
CL_{bile_AG}	285 ± 37	1.67 ± 0.21*
CL_{bile_AS}	106 ± 12	16 ± 1*
CL_{B/L_AG}	289 ± 107	2110 ± 359*
CL_{B/L_AS}[b]	2575 ± 260	1510 ± 130*

[a] Mean ± S.D., $n = 3$ for each group.
[b] Apparent as basolateral clearance.
* $P < 0.01$, control vs. TR⁻.

in Sf9 cells were validated by determining the uptake of TC and $E_2 17\beta G$ into Mrp2- or Mrp3-expressing Sf9 cell PMVs, respectively (data not shown). Net ATP-dependent [^{3}H]TC and [^{3}H]$E_2 17\beta G$ uptake was very low in control (GFP-expressing Sf9 cell plasma membrane) vesicles. Significantly higher net ATP-dependent uptake of [^{3}H]TC into Mrp3-expressing Sf9 cell PMVs compared with control vesicles was observed. Likewise, net ATP-dependent [^{3}H]$E_2 17\beta G$ uptake into Mrp2-expressing Sf9 cell PMVs was significantly higher than the control vesicles.

Net ATP-dependent uptake of AG by Mrp3 expressed in Sf9 cell PMVs through 10 min is shown in Figure 3A. AG uptake into control and Mrp3-expressing Sf9 cell PMVs at 5 min was determined in the presence of 10 to 600 μM AG, and the Michaelis-Menten equation was fit to the net ATP-dependent Mrp3-mediated AG uptake versus concentration data (Fig. 3B). The estimated V_{max} was 2.1 ± 0.2 nmol/min/mg of protein, and the estimated K_m was 0.91 ± 0.10 mM (mean ± S.E.). Although the K_m cannot be estimated precisely based on the substrate concentration range used in this study, it does indicate that AG is a low-affinity substrate of Mrp3.

No net ATP-dependent AG uptake was observed up to 45 min with Mrp2-expressing Sf9 cell PMVs (data not shown). Addition of 5 mM glutathione to the uptake buffer did not stimulate AG uptake into Mrp2-expressing Sf9 cell PMVs. The interaction of AG with Mrp2 was studied indirectly by determining the inhibition of Mrp2-mediated CDF transport by AG. Uptake of 10 μM CDF into Mrp2-expressing Sf9 cell PMVs was almost linear up to 10 min; endogenous CDF uptake activity in control (GFP-expressing) vesicles was negligible. CDF uptake into control and Mrp2-expressing Sf9 cell PMVs at 5 min was determined in the presence of 5 to 500 μM CDF (Fig. 4A), and the Michaelis-Menten equation was fit to the net ATP-dependent Mrp2-mediated CDF uptake versus concentration data. The estimated V_{max} and K_m values from three independent studies were 1.4 ± 0.5 nmol/min/mg of protein and 0.14 ± 0.02 mM, respectively (mean ± S.D.).

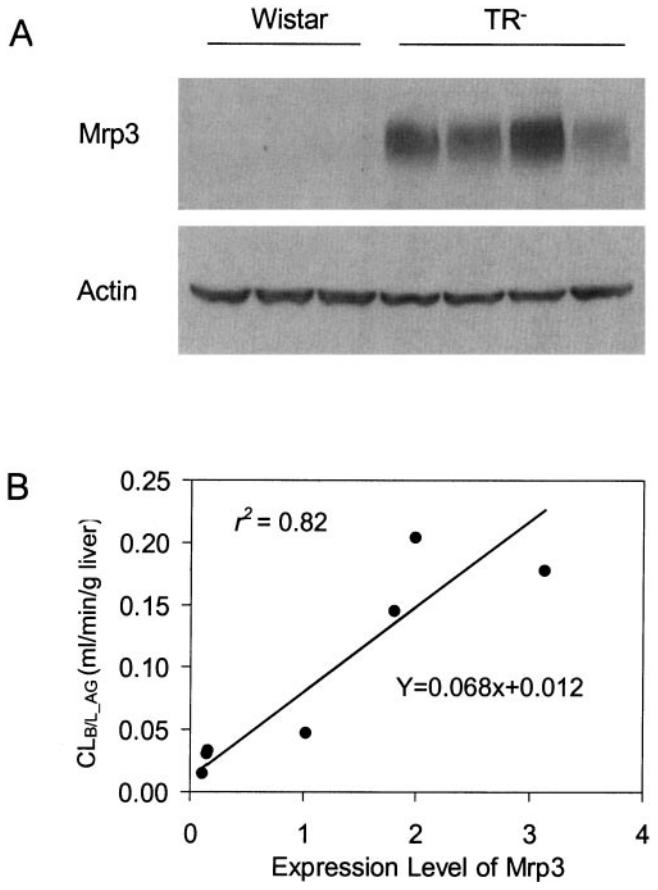

FIG. 2. *Expression of Mrp3 in Wistar and TR⁻ rat livers (A) and correlation between AG basolateral clearance and Mrp3 expression in these livers (B).*

The straight line represents the best fit to the data based on orthogonal linear regression. Expression levels of Mrp3 shown in (B) were normalized by the levels of actin in each liver.

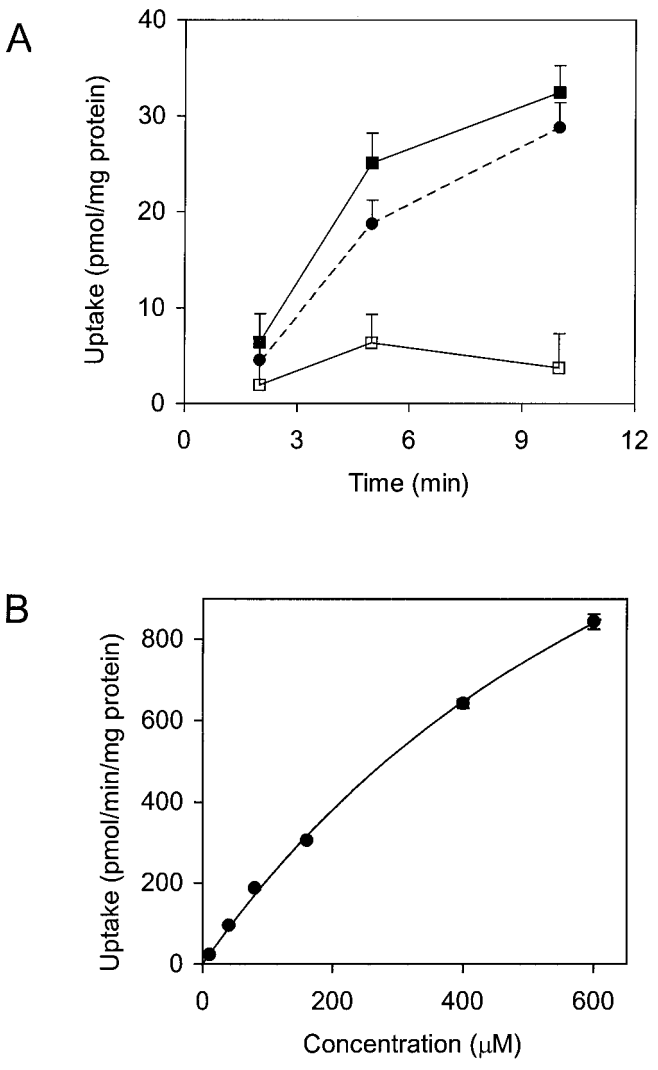

FIG. 3. *Time course (A) and concentration dependence (B) of [³H]AG uptake by Mrp3 expressed in Sf9 cells.*

A, net ATP-dependent uptake of 10 μM AG into Mrp3-expressing (■) and control (GFP-expressing; □) Sf9 cell PMVs were determined as the difference between the uptake in the presence of 4 mM ATP and AMP. Mrp3-mediated uptake of AG (●) was determined as the difference between net ATP-dependent uptake into Mrp3-expressing and control Sf9 cell PMVs. B, concentration-dependent AG uptake by Mrp3 at 5 min was determined in the presence of 10 to 600 μM AG. The curve represents the best fit of the Michaelis-Menten equation to the data. Data represent mean ± S.D. (n = 3).

Inhibition Studies. Mrp2-mediated CDF uptake was modestly but statistically significantly inhibited by 0.5 and 1 mM AG (Fig. 4B). Assuming a simple competitive mechanism of inhibition, the K_i was estimated roughly to be ~4 to 5 mM, consistent with the hypothesis that AG is an extremely low affinity Mrp2 substrate.

As shown in Fig. 5, PB (1 mM) had no effect on Mrp2-mediated CDF uptake or Mrp3-mediated AG uptake. *p*-OHPB (1 mM) significantly inhibited Mrp2 but not Mrp3 activity. *p*-OHPBG significantly inhibited both Mrp2-mediated CDF uptake and Mrp3-mediated AG uptake at 0.5 mM ($P < 0.05$). The inhibition of Mrp2-mediated CDF uptake and Mrp3-mediated AG uptake by *p*-OHPBG was studied further in the presence of 0 to 1 mM *p*-OHPBG (Fig. 6). Estimated IC_{50} values for *p*-OHPBG were 0.68 ± 0.02 and 0.46 ± 0.03 mM (mean ± S.E.) for the inhibition of Mrp2-mediated CDF uptake and Mrp3-mediated AG uptake, respectively. Estimated n values for the inhibition of Mrp2-mediated CDF uptake and Mrp3-mediated AG uptake by *p*-OHPBG were 2.9 and 1.9, respectively.

PB Induction of Mrp3. Western blot analysis revealed that the constitutive expression level of Mrp3 protein in Wistar rat livers was very low. After PB treatment for 4 days followed by a 24-hour washout period, Mrp3 protein was significantly induced (>10-fold). In contrast, PB treatment did not alter Mrp2 levels (Fig. 7).

Discussion

AG undergoes biliary excretion and basolateral export to a similar extent in rats. Assuming that AG formation is not altered, decreased biliary excretion of AG due to PB treatment can be attributed to either an impairment in biliary excretion or an up-regulation in basolateral export of AG. The present study examined the hypothesis that alterations in AG biliary and basolateral transport processes are responsible for the impaired biliary excretion of AG after PB pretreatment or acute treatment with PB.

First of all, the major transport systems responsible for the biliary excretion and basolateral export of AG were investigated. Previous pharmacokinetic modeling and simulation studies suggested that the biliary excretion of AG is mediated almost exclusively by Mrp2 and that Mrp3 is involved in basolateral export of AG (Xiong et al., 2000). These findings were supported further by data from single-pass isolated perfused Wistar and TR⁻ rat livers. During single-pass perfusion, the biliary and basolateral clearance of a drug can be calculated directly from the biliary excretion rate, basolateral export rate, and the intrahepatic drug concentration at steady-state, assuming that the liver

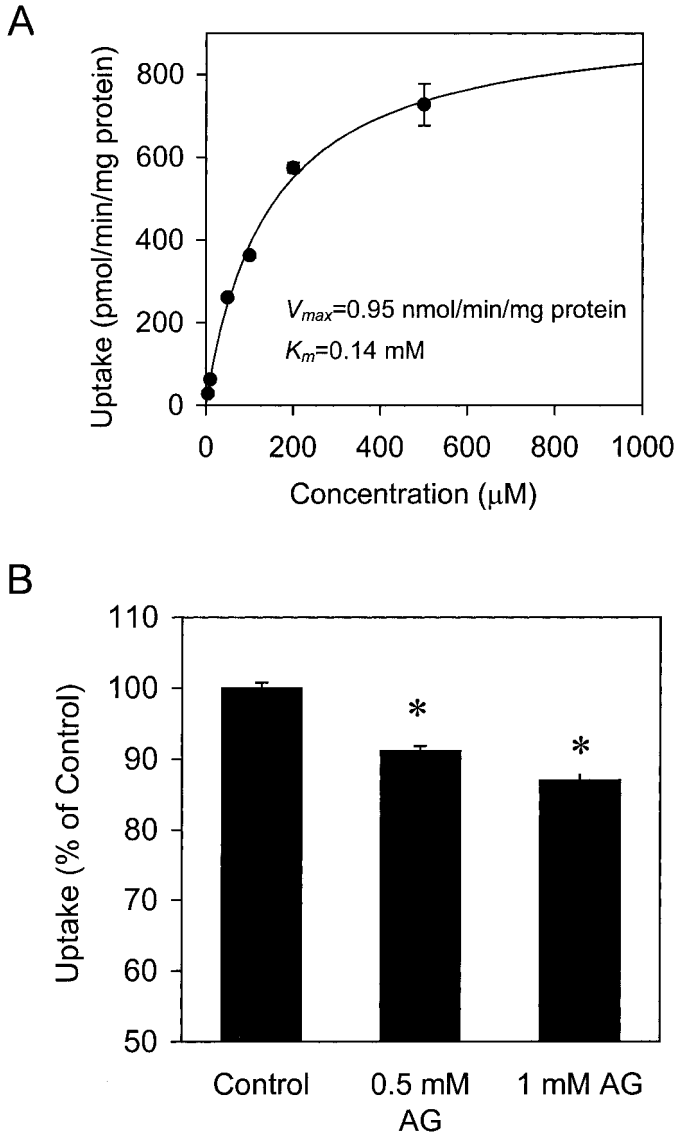

FIG. 4. *Concentration-dependence (A) and AG inhibition (B) of CDF uptake by Mrp2 expressed in Sf9 cells.*

A, concentration-dependent CDF uptake by Mrp2 at 5 min was determined as the difference between net ATP-dependent uptake into Mrp2-expressing and control Sf9 cell PMVs in the presence of 5 to 500 μM CDF. The curve represents the best fit of the Michaelis-Menten equation to the data. B, Mrp2-mediated CDF uptake was determined as the difference between the net ATP-dependent uptake of 10 μM CDF into Mrp2-expressing and control Sf9 cell PMVs at 5 min at 37°C. Data represent mean ± S.D. (n = 3); *, $P < 0.01$.

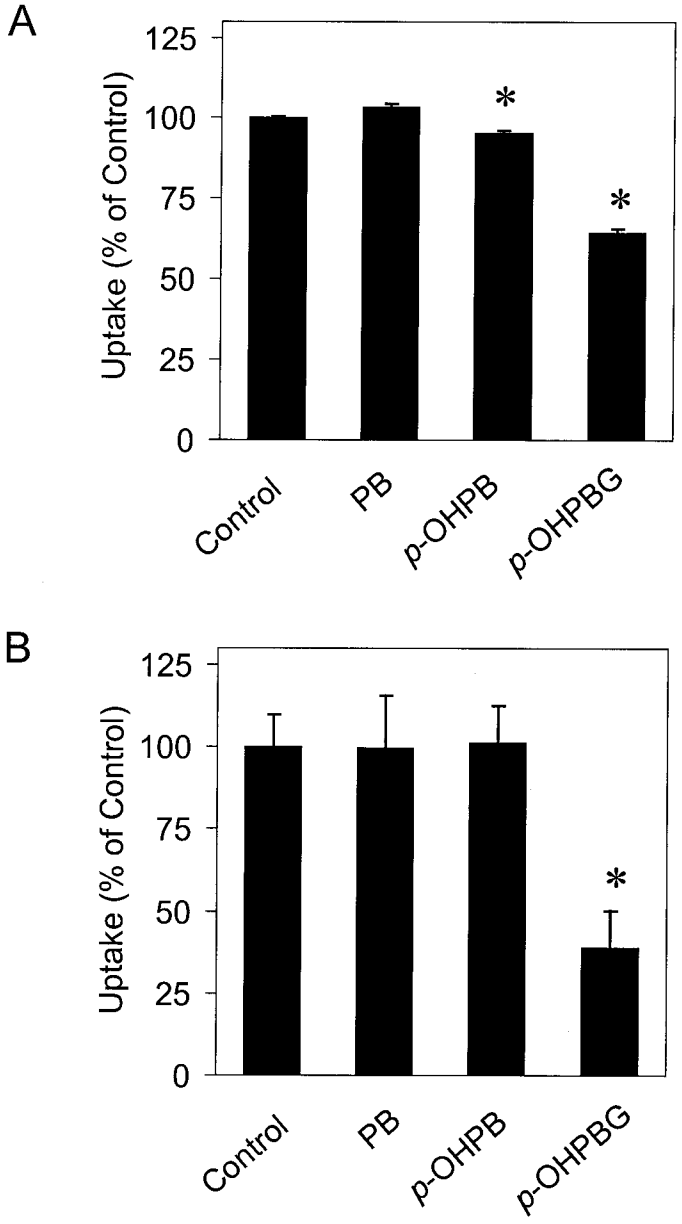

FIG. 5. *Inhibition of Mrp2-mediated CDF uptake (A) and Mrp3-mediated [^{3}H]AG uptake (B) by PB, p-OHPB, and p-OHPBG.*

A, Mrp2-mediated CDF uptake was determined as the difference between the net ATP-dependent uptake of 10 μM CDF into Mrp2-expressing and that into GFP-expressing Sf9 cell PMVs for 5 min at 37°C (n = 3). B, Mrp3-mediated [^{3}H]AG uptake was determined as the difference between the net ATP-dependent uptake of 10 μM AG into Mrp3-expressing and that into GFP-expressing Sf9 cell PMVs for 5 min at 37°C (n = 3). Concentrations of PB, *p*-OHPB, and *p*-OHPBG were 1, 1, and 0.5 mM, respectively. *, $P < 0.01$.

is a well stirred compartment and the transport processes are unidirectional (Takenaka et al., 1995). Consistent with the results from the pharmacokinetic modeling and simulation studies (Xiong et al., 2000), the biliary clearance of AG and AS (CL_{bile_AG} and CL_{bile_AS}) in TR$^-$ rat livers was ~170- and ~7-fold lower than in Wistar rat livers, respectively, the basolateral clearance of AG (CL_{B/L_AG}) was ~7-fold higher in TR$^-$ relative to Wistar rat livers, and the steady-state AG concentrations were significantly lower in TR$^-$ compared with Wistar rat livers (Table 1). The single-pass perfusion study only allowed calculation of the apparent basolateral clearance of AS (CL_{B/L_AS}) because AS is taken up as well as excreted across the basolateral membrane of the hepatocyte (Iida et al., 1989; Sakuma-Sawada et al., 1997; Xiong et al., 2000), thus violating the assumption of unidirectional transport in analysis of single-pass perfusion data. In contrast, hepatic uptake of AG is negligible (Liu and Brouwer, 1995), which is consistent with the high K_m and low V_{max} values reported by Iida et al. (1989). The almost complete absence of AG biliary excretion in TR$^-$ rat livers indicates that the biliary excretion of AG is mediated primarily by Mrp2. The up-regulation of Mrp3 in TR$^-$ rat livers, and the significant correlation (r^2 = 0.82) between the basolateral clearance of AG and the expression level of Mrp3 in control and TR$^-$ rat livers, suggest that Mrp3 plays a key role in the basolateral export of AG to compensate for the loss of Mrp2 function in TR$^-$ rat livers. The positive *y*-axis intercept of the best-fit line describing the relationship between the basolateral clearance of AG and the expression level of

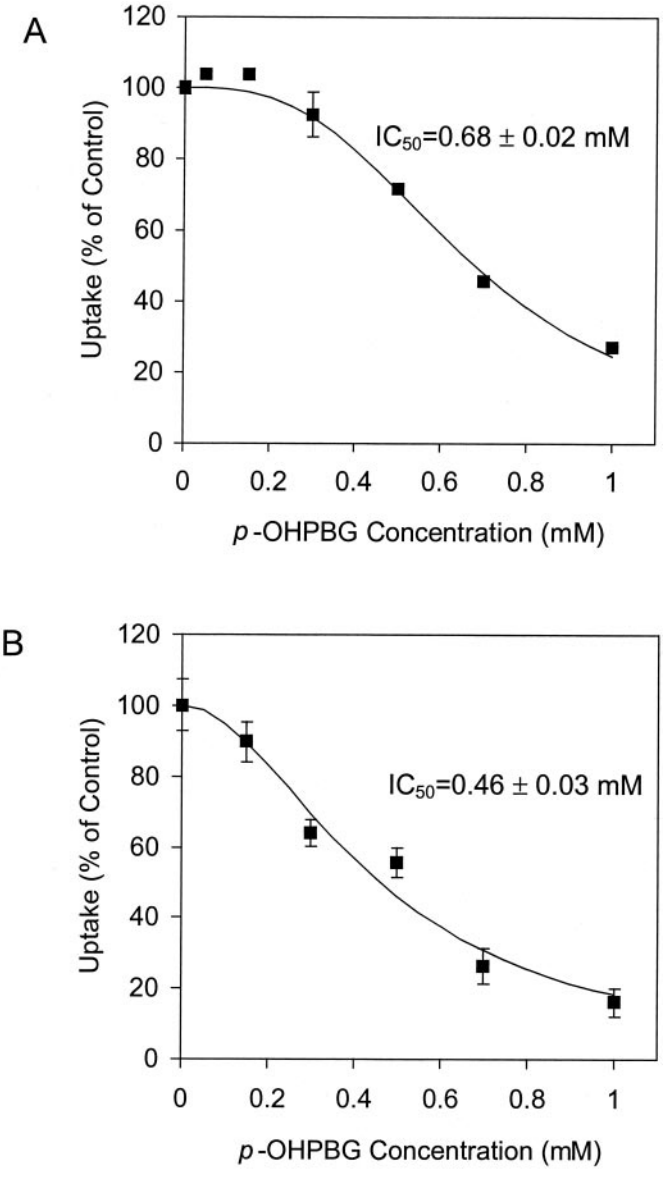

FIG. 6. *Concentration-dependent inhibition of Mrp2-mediated CDF uptake (A) and Mrp3-mediated [^{3}H]AG uptake (B) by p-OHPBG.*

A, Mrp2-mediated CDF uptake was determined as the difference between the net ATP-dependent uptake of 10 μM CDF into Mrp2-expressing and control Sf9 cell PMVs for 5 min at 37°C (mean ± S.D.; $n = 3$). B, Mrp3-mediated AG uptake was determined as the difference between the net ATP-dependent uptake of 10 μM AG into Mrp3-expressing and control Sf9 cell PMVs for 5 min at 37°C (mean ± S.D.; $n = 3$). The curves represent the best fit of equation (5) to the data in each study. IC_{50} values represent mean ± S.E. as reported by WinNonlin.

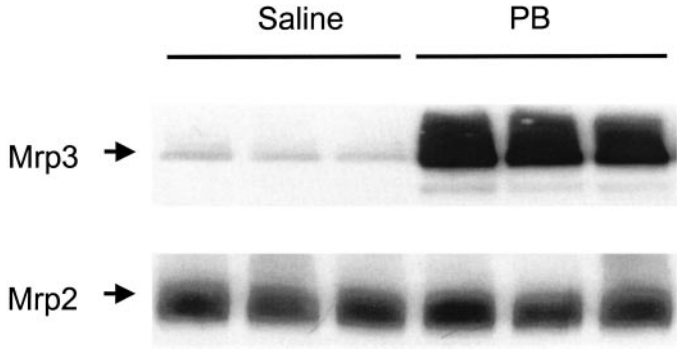

FIG. 7. *Induction of Mrp3 protein by PB pretreatment.*

Liver crude membrane fractions (60 μg of protein) prepared from Wistar rats treated for 4 days with saline or PB, followed by a 24-hour washout period, were separated on 4 to 12% Bis-Tris polyacrylamide gels, transferred to PVDF membrane, and probed with anti-Mrp3 and anti-Mrp2 antiserum separately.

Mrp3 (Fig. 2) would be consistent with the presence of other transporter(s) involved in the basolateral export of AG. Increased basolateral efflux clearance of E3040 glucuronide and TC have been observed in Eisai hyperbilirubinemic rats (Takenaka et al., 1995; Akita et al., 2001), which is consistent with the up-regulation of hepatic Mrp3 in these rats (Hirohashi et al., 1998; Ogawa et al., 2000). Taken together, these reports suggest that the up-regulation of Mrp3 in Mrp2-deficient rat livers provides a general mechanism by which hepatocytes avoid the accumulation of organic anions.

Uptake studies with Mrp3-expressing Sf9 cell PMVs clearly demonstrated that AG is a low-affinity Mrp3 substrate. Single-pass liver perfusion studies suggested that Mrp3 plays a key role in the basolateral export of AG in TR$^-$ rat livers. However, to what extent Mrp3 contributes to the basolateral export of AG in normal Wistar rat livers is unknown. Single-pass liver perfusion studies suggest that there may be other transporter(s) involved in the basolateral export of AG. Mrp1 has overlapping substrate specificity with Mrp3. However, Mrp1 expression in normal rat livers is not detectable (Ogawa et al., 2000). Thus, the potential role of Mrp1 in mediating AG basolateral export probably is negligible. Several ATP-independent organic anion transporters have been identified in rat hepatic basolateral membranes, including all four members of the rat Oatp family (Oatp 1–4) and two members of the rat organic anion transporter family (Oat2 and 3) (Kullak-Ublick, 1999; Cattori et al., 2000). However, the functional characterization of these transporters, which are thought to be predominantly hepatic uptake transporters, remains incomplete. Little is known about the role of these transport proteins in hepatic basolateral export of organic anions. Recently, in vitro studies suggested that Oatp transporters could mediate bidirectional transport of some organic anions (Shi et al., 1995; Satlin et al., 1997; Li et al., 1998, 2000). Additional studies are needed to clarify the relative role of Mrp3 in AG basolateral export in normal rat livers and to determine what other transporters are involved in the export of AG across the hepatic basolateral membrane.

Net ATP-dependent AG uptake into Mrp2-expressing Sf9 cell PMVs was not detected. However, AG inhibited Mrp2-mediated CDF uptake. Based on the observation that AG is a weak inhibitor of Mrp2-mediated CDF uptake, the undetectable net ATP-dependent uptake of AG by Mrp2-expressing Sf9 cell PMVs was likely due to the extremely low affinity of AG for Mrp2 ($K_i = \sim 4–5$ mM). In previous studies, net ATP-dependent AG uptake was barely measurable in canalicular liver plasma membrane vesicles (Xiong et al., 2000). So far, the weakest substrates that have been reported for rat Mrp2 and human MRP2 are methotrexate ($K_m = 295$ μM) and *p*-aminohippurate ($K_m = 880$ μM), respectively (Masuda et al., 1997; Leier et al., 2000). The estimated K_m of AG for Mrp3 is ~0.91 mM, which is lower than the K_i estimated for AG inhibition of Mrp2-mediated CDF transport. The higher affinity of AG for Mrp3 than for Mrp2 suggests that Mrp3 could play a key role in the basolateral export of AG despite the fact that the expression level of Mrp3 is substantially lower than Mrp2 in Wistar rat livers.

PB, *p*-OHPB and *p*-OHPBG are the major species found in bile after a dose of PB (Levin et al., 1986). Among them, only *p*-OHPBG markedly inhibited Mrp2-mediated CDF uptake. AG biliary excretion is mediated almost exclusively by Mrp2 (Xiong et al., 2000). The importance of *p*-OHPBG-mediated inhibition of AG biliary excretion to the overall hepatobiliary disposition of AG after acute PB treatment

depends on the relative role of Mrp3 in the basolateral export of AG. *p*-OHPBG inhibited Mrp2-mediated CDF uptake and Mrp3-mediated AG uptake with similar potency. If Mrp3 is the primary AG basolateral export transporter, *p*-OHPBG would inhibit AG biliary excretion and basolateral export to a similar degree, and the cumulative amount of AG excreted in bile through time infinity would show no or little change due to *p*-OHPBG inhibition. If other transporter(s) also contribute significantly to AG basolateral export, and exhibit less or no inhibition by *p*-OHPBG, *p*-OHPBG would preferentially inhibit AG biliary excretion, resulting in decreased AG appearance in bile.

PB has a relatively short half-life (~9 h) in vivo in rats (Brouwer et al., 1984). For rats pretreated with PB in the previous studies, by the time APAP was administered (24 or 48 h after the last dose of PB), most PB and PB metabolites should have been eliminated from the body (Brouwer and Jones, 1990; Studenberg and Brouwer, 1992). Thus, the direct inhibition of AG biliary excretion by PB metabolites probably plays a minor role in the impaired biliary excretion of AG after PB pretreatment. However, the effects of PB on the expression of hepatobiliary transporters must be considered. Marked induction of Mrp3 (>10-fold) and no significant change in the expression of Mrp2 in Wistar rat livers after 4 days of PB treatment observed in the present study were consistent with a previous report in Sprague-Dawley rats (Ogawa et al., 2000). Effects of PB treatment on some other basolateral organic anion transporters also have been examined in Sprague-Dawley rats. PB treatment for 4 days did not alter the expression of Mrp1 or Oatp1 (Ogawa et al., 2000). A moderate induction of Oatp2 (less than 2-fold) by PB has been reported (Rausch-Derra et al., 2001). Simulation studies have shown that a 10-fold increase in the basolateral export rate constant is needed to cause a ~5-fold reduction in the biliary excretion of AG (Xiong et al., 2000), which is about the extent of impairment in the biliary excretion of AG by PB pretreatment. Thus, even if Oatp2 transports AG, the induction of Mrp3 instead of Oatp2 appears to be the primary cause of the impaired biliary excretion of AG after PB pretreatment.

In conclusion, the present study demonstrated that the biliary and basolateral clearances of AG and/or AS calculated based on data from single-pass perfused rat livers were comparable with those estimated by pharmacokinetic modeling (Xiong et al., 2000). AG is a low-affinity substrate for Mrp2 and Mrp3. *p*-OHPBG, a major metabolite of PB, significantly inhibited Mrp2- and Mrp3-mediated transport processes. PB pretreatment (80 mg/kg/day for 4 days followed by a 24-hour washout period) markedly induced hepatic Mrp3 whereas it had no significant effect on Mrp2 expression in Wistar rats. These results suggest that impaired biliary excretion of AG after PB pretreatment may be attributed primarily to the induction of hepatic Mrp3. In addition to the moderate decrease in AG formation (Studenberg and Brouwer, 1992), impaired biliary excretion of AG after acute PB treatment also may be attributed to the preferential inhibition of Mrp2-mediated AG biliary excretion by *p*-OHPBG over AG basolateral export processes (only one of which is inhibited by *p*-OHPBG).

References

Akita H, Suzuki H, and Sugiyama Y (2001) Sinusoidal efflux of taurocholate is enhanced in Mrp2-deficient rat liver. *Pharm Res (NY)* **18:**1119–1125.

Bergwerk AJ, Shi X, Ford AC, Kanai N, Jacquemin E, Burk RD, Bai S, Novikoff PM, Stieger B, Meier PJ, Schuster VL, and Wolkoff AW (1996) Immunologic distribution of an organic anion transport protein in rat liver and kidney. *Am J Physiol* **271:**G231–G238.

Brouwer KL and Jones JA (1990) Altered hepatobiliary disposition of acetaminophen metabolites after phenobarbital pretreatment and renal ligation: evidence for impaired biliary excretion and a diffusional barrier. *J Pharmacol Exp Ther* **252:**657–664.

Brouwer KL, Kostenbauder HB, McNamara PJ, and Blouin RA (1984) Phenobarbital in the genetically obese Zucker rat. I. Pharmacokinetics after acute and chronic administration. *J Pharmacol Exp Ther* **231:**649–653.

Cattori V, Hagenbuch B, Hagenbuch N, Stieger B, Ha R, Winterhalter KE, and Meier PJ (2000) Identification of organic anion transporting polypeptide 4 (Oatp4) as a major full-length isoform of the liver-specific transporter-1 (rlst-1) in rat liver. *FEBS Lett* **474:**242–245.

Hirohashi T, Suzuki H, Ito K, Ogawa K, Kume K, Shimizu T, and Sugiyama Y (1998) Hepatic expression of multidrug resistance-associated protein-like proteins maintained in Eisai hyperbilirubinemic rats. *Mol Pharmacol* **53:**1068–1075.

Huang L, Hoffman T, and Vore M (1998) Adenosine triphosphate-dependent transport of estradiol-17beta(beta-D-glucuronide) in membrane vesicles by MDR1 expressed in insect cells. *Hepatology* **28:**1371–1377.

Iida S, Mizuma T, Sakuma N, Hayashi M, and Awazu S (1989) Transport of acetaminophen conjugates in isolated rat hepatocytes. *Drug Metab Dispos* **17:**341–344.

Ito K, Suzuki H, and Sugiyama Y (2001) Charged amino acids in the transmembrane domains are involved in the determination of the substrate specificity of rat Mrp2. *Mol Pharmacol* **59:**1077–1085.

Kullak-Ublick GA (1999) Regulation of organic anion and drug transporters of the sinusoidal membrane. *J Hepatol* **31:**563–573.

Leier I, Hummel-Eisenbeiss J, Cui Y, and Keppler D (2000) ATP-dependent para-aminohippurate transport by apical multidrug resistance protein MRP2. *Kidney Int* **57:**1636–1642.

Levin SS, Vars HM, Schleyer H, and Cooper DY (1986) The metabolism and excretion of enzyme-inducing doses of phenobarbital by rats with bile fistulas. *Xenobiotica* **16:**213–224.

Li L, Lee TK, Meier PJ, and Ballatori N (1998) Identification of glutathione as a driving force and leukotriene C4 as a substrate for oatp1, the hepatic sinusoidal organic solute transporter. *J Biol Chem* **273:**16184–16191.

Li L, Meier PJ, and Ballatori N (2000) Oatp2 mediates bidirectional organic solute transport: a role for intracellular glutathione. *Mol Pharmacol* **58:**335–340.

Liu X and Brouwer KLR (1995) Acetaminophen glucuronide disposition in the isolated perfused rat liver: effects of phenobarbital. *Pharm Res (NY)* **12:**S-386 (8237).

Masuda M, I'Izuka Y, Yamazaki M, Nishigaki R, Kato Y, Ni'inuma K, Suzuki H, and Sugiyama Y (1997) Methotrexate is excreted into the bile by canalicular multispecific organic anion transporter in rats. *Cancer Res* **57:**3506–3510.

Ogawa K, Suzuki H, Hirohashi T, Ishikawa T, Meier PJ, Hirose K, Akizawa T, Yoshioka M, and Sugiyama Y (2000) Characterization of inducible nature of MRP3 in rat liver. *Am J Physiol* **278:**G438–G446.

Rausch-Derra LC, Hartley DP, Meier PJ, and Klaassen CD (2001) Differential effects of microsomal enzyme-inducing chemicals on the hepatic expression of rat organic anion transporters, OATP1 and OATP2. *Hepatology* **33:**1469–1478.

Sakuma-Sawada N, Iida S, Mizuma T, Hayashi M, and Awazu S (1997) Inhibition of the hepatic uptake of paracetamol sulphate by anionic compounds. *J Pharm Pharmacol* **49:**743–746.

Satlin LM, Amin V, and Wolkoff AW (1997) Organic anion transporting polypeptide mediates organic anion/HCO_3^- exchange. *J Biol Chem* **272:**26340–26345.

Shi X, Bai S, Ford AC, Burk RD, Jacquemin E, Hagenbuch B, Meier PJ, and Wolkoff AW (1995) Stable inducible expression of a functional rat liver organic anion transport protein in HeLa cells. *J Biol Chem* **270:**25591–25595.

Studenberg SD and Brouwer KL (1992) Impaired biliary excretion of acetaminophen glucuronide in the isolated perfused rat liver after acute phenobarbital treatment and in vivo phenobarbital pretreatment. *J Pharmacol Exp Ther* **261:**1022–1027.

Studenberg SD and Brouwer KL (1993) Hepatic disposition of acetaminophen and metabolites. Pharmacokinetic modeling, protein binding and subcellular distribution. *Biochem Pharmacol* **46:**739–746.

Studenberg SD, Price-Raybuck DL, Unger SE, Shockcor J, and Brouwer KL (1995) Characterization of *p*-hydroxyphenobarbital glucuronide generated from immobilized rat hepatic UDP-glucuronosyltransferase. *J Pharm Sci* **84:**1134–1136.

Takenaka O, Horie T, Kobayashi K, Suzuki H, and Sugiyama Y (1995) Kinetic analysis of hepatobiliary transport for conjugated metabolites in the perfused liver of mutant rats (EHBR) with hereditary conjugated hyperbilirubinemia. *Pharm Res (NY)* **12:**1746–1755.

Tsuji A, Yoshikawa T, Nishide K, Minami H, Kimura M, Nakashima E, Terasaki T, Miyamoto E, Nightingale CH, and Yamana T (1983) Physiologically based pharmacokinetic model for beta-lactam antibiotics I: Tissue distribution and elimination in rats. *J Pharm Sci* **72:**1239–1252.

Turner KC and Brouwer KL (1997) In vitro mechanisms of probenecid-associated alterations in acetaminophen glucuronide hepatic disposition. *Drug Metab Dispos* **25:**1017–1021.

Vore M, Hoffman T, and Gosland M (1996) ATP-dependent transport of beta-estradiol 17-(beta-D-glucuronide) in rat canalicular membrane vesicles. *Am J Physiol* **271:**G791–798.

Xiong H, Turner KC, Ward ES, Jansen PL, and Brouwer KL (2000) Altered hepatobiliary disposition of acetaminophen glucuronide in isolated perfused livers from multidrug resistance-associated protein 2-deficient TR(−) rats. *J Pharmacol Exp Ther* **295:**512–518.